On the Evaluation of Stability of Rare Earth Oxides as Face Coats for Investment Casting of Titanium

R.L. SAHA, T.K. NANDY, R.D.K. MISRA, and K.T. JACOB

Attempts have been made to evaluate the thermal stability of rare earth oxide face coats against liquid titanium. Determination of microhardness profiles and concentration profiles of oxygen and metallic constituents of oxide in investment cast titanium rods has allowed gradation of relative stability of rare earth oxides. The relative stability of evaluated oxides in the order of increasing stability follows the sequence $CeO_2 \rightarrow ZrO_2 \rightarrow Gd_2O_3 \rightarrow$ didymium oxide $\rightarrow Sm_2O_3 \rightarrow Nd_2O_3 \rightarrow Y_2O_3$. The grading does not follow the free energy data of the formation of these oxides. A better correlation with the experimental observations is obtained when the solubility of the metallic species in titanium is also taken into consideration.

I. INTRODUCTION

INVESTMENT casting provides a high degree of dimensional tolerance (0.4 to 1.6 mm) and surface finish (0.8 to 3.8 μm), which are far superior than those obtained in sand castings.[1,2,3] Investment castings also provide design flexibility to produce highly intricate shapes. The molds for investment casting are produced from refractory slurries containing finely divided materials for obtaining good surface finishes. Refractories used in investment molds are relatively more stable and inert compared to those required for sand casting.

A number of studies have been carried out on the reactivity of titanium with a variety of refractory materials including borides, carbides, sulfides, nitrides, and oxides. Borides of Cr, Ti, W, and Zr were found to severely contaminate the titanium melt.[4] Among the Cr, Mo, Ta, and Ti borides, TaB_2 caused the least amount of contamination of molten titanium.[5] In general, borides do not offer much promise as a mold face coat material and, thus, have not been actively pursued.

Titanium carbide formation was observed in all castings using crucibles made of carbides of elements B, Mo, Si, Ta, Ti, W, and Zr.[4] It appears that the affinity of titanium for carbon triumphs even over the most stable carbides. NbC performed satisfactorily while in contact with molten titanium, probably because of a slower rate of carbon diffusion.[6] Nitrides of refractory elements were also found to severely contaminate the melt.[4] As regards the performance of sulfides, computer calculations have shown significant advantages in the use of sulfides as mold coatings for titanium castings. Sulfides of calcium and magnesium were not satisfactory since appreciable pressure of metallic elements develops in equilibrium with molten titanium. The rare earth sulfides were found to perform better.

Oxyfluorides have recently been investigated, and some have proven effective. Neodymium oxyfluoride[7] and lanthanum oxyfluoride[8] have been patented as the major constituents in a mold coating. However, oxysulfides or oxyfluorides need to be prepared carefully to ensure purity and correct stoichiometry.

In search of suitable mold material, the oxide family of materials has received the most attention. The free energy diagram for oxides is useful for comparison of the relative stability of oxides.[9] The general reaction represented on the diagram is

$$2\frac{x}{y}\,M\,(s, l, \text{or } g) + O_2\,(g) \rightarrow \frac{2}{y}\,M_xO_y\,(s, l, \text{or } g) \quad [1]$$

Since only the standard free energy is plotted, the diagram does not provide a correct picture of the reactivity of oxides with liquid titanium. Solution effects need to be taken into consideration to obtain a more realistic picture. In an early study, zirconia was found to be the least reactive of the various oxides examined.[4] Later investigations[10,11] indicated that Y_2O_3 or HfO_2 stabilized zirconia (ZrO_2) had performed better than CaO-stabilized ZrO_2. Pure Y_2O_3 has received considerable attention by investigators,[12–16] with Y_2O_{3-x} and Y_2O_3 + 8 to 15 wt pct Ti performing the best. Yttria, however, is fairly expensive; therefore, it would be desirable to use it as an additive or only in selected mold sections. Its addition improves the performance of other materials such as ZrO_2 and Al_2O_3. Rare earth oxides have also been the subject of interest,[11,12,16,17] with some positive results. However, the major drawback is their cost.

In the present study, various rare earth oxide face coats have been evaluated on zircon sand investment molds as it has been difficult to quantify the chemical reactivity of titanium with the constituents of mold to date. An attempt is made here to quantify the performance of each of the face coats by determination of microhardness and diffusion profiles of constituent elements. The experimental data on the extent of contamination have been compared with the phase stability and thermodynamic data.

II. EXPERIMENTAL

A. *Preparation of Investment Molds*

The wax pattern was made by injecting wax into a simple cylindrical metal mold (20-mm diameter ×

R.L. SAHA, Deputy Director, T.K. NANDY, Scientist, and R.D.K. MISRA, Scientist, are with the Defence Metallurgical Research Laboratory, P.O. Kanchanbagh, Hyderabad 500 258, India. K.T. JACOB, Chairman, is with the Department of Metallurgy, Indian Institute of Science, Bangalore 560 012, India.

Manuscript submitted September 13, 1989.

100 mm) with an integral pouring basin. Wax patterns were then inspected and dressed to eliminate any imperfections resulting from injection. The pattern was dip-coated with a primary slurry coat containing very fine particles of required oxide and colloidal silica. It was then stuccoed after draining the excess slurry and given another coat with the same slurry. Later stuccoing was done with coarser zircon sand or alumina powder, and the shell thickness of ~3 mm was built with alternating dipping and stuccoing. The shells were dried at controlled temperature (295± K) and relative humidity (50 ± 10 pct) for at least 24 hours. This was followed by dewaxing in an autoclave at about 440 K at a pressure of about 0.5 MPa (80 psi) and then firing at 1123 K.

B. *Melting and Casting of Titanium*

A drop casting hearth suitable for the melting of about a 200 g charge by a nonconsumable tungsten electrode was designed for use in a 40 kg vacuum arc furnace. The design of this drop casting hearth is described in an earlier work.[18]

The charge of commercially pure titanium buttons was placed on the drop cast hearth by first placing a titanium disc at the bottom for blocking the pouring nozzle and then closing the furnace. The vacuum furnace was evacuated to 0.133 Pa (10^{-3} torr) and refilled with argon to 5.32×10^4 Pa (400 mm) pressure. This cycle of evacuation and flushing with argon was repeated at least two times. The charge consisted of cut pieces, approximately 20 × 10 mm in size, from a titanium rod or buttons of known purity. Melting was initiated by striking an arc (300 to 400 A) against the charge with a thoriated tungsten electrode. The melting current was then raised to 700 A. When the charge was in fully molten condition, the arc was directed at the center of the hearth to melt the titanium disc, thereby allowing the liquid metal to flow into the mold positioned below the hearth. After sufficient cooling, the crucible was removed from the furnace and the cast rod (20-mm diameter × 100 mm) taken out of the mold. The operating parameters were standardized after extensive trials.

C. *Determination of the Diffusion Profiles of Oxygen and Rare Earth Elements*

Secondary ion mass spectrometry (SIMS) was used to determine the diffusion depth of oxygen and some of the rare earth elements. For obtaining the concentration profiles of oxygen and rare earth elements, samples were prepared from the cast titanium rods. The analysis of oxygen was performed using Cs bombardment and collecting the negative secondary ions. The sample was moved step by step under the primary beam from the edge (metal-mold interface) toward the center for a distance of 1.0 mm. The signals for the ions O^{16-} and Ti^{48-} were recorded at each position of the sample. The primary current used was 3.5 mA at 10 kV, and the beam intensity was 792 nA. The analyzed area was 8.33 μm in diameter, and the mass resolving power used was 300.

The analyses of Y and Nd were performed under O_2 bombardment. The positive secondary ions were collected. The samples coming from the shells containing Al_2O_3 as backup sand exhibited molecular ions TiA at mass 89, interfering with Y. To eliminate this ir ference, two methods were used: energy filtering and mass resolution. In the case of Y, both methods g good agreement. The Nd profiles were obtained by u energy filtering to avoid interferences with molecular Ti_3^+ and $Ti_2O_3^+$. In all of the cases, the primary beam arc current used was 54.4 mA at 15 kV. The lyzed area was 8.33 μm in diameter, and the mas solving power used was 3600 for Y and 300 for analysis.

D. *Heating Titanium in Contact with Different Face Coat Oxides above Its Melting Point*

The oxides of various elements were heated in cor with titanium above its melting point to obtain an i cation of the solubility of these oxides in liquid titani A commercially pure titanium rod (6-mm diamete placed at the center of a graphite crucible (10-mm ameter × 20 mm) over a layer of the oxide under vestigation, and the annular space between the rod the crucible is rammed with the same oxide. A nur of such graphite crucibles with different oxides were kept in a graphite block provided with a number of for this purpose (Figure 1). The graphite block, a with the crucibles, is then heated to the de temperature above the melting point in a graphite uum resistance heating furnace (Advanced Vac

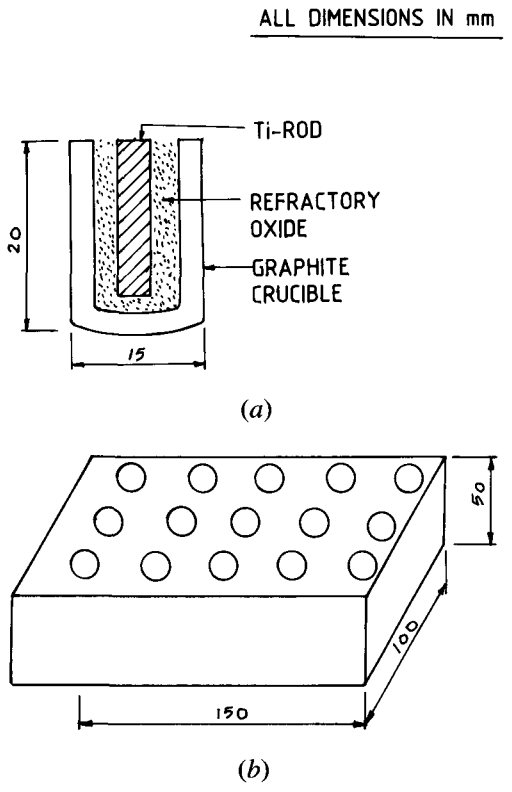

Fig. 1 — Setup for heating rare earth oxides along with titanium a its melting point: (*a*) schematic arrangement of refractory oxide p around titanium rod in a graphite crucible and (*b*) graphite blo accommodate 15 crucibles.

System, MA). The pressure in the furnace was of the order of 1.33×10^{-3} Pa. The furnace was heated at a rate of ~10 K/s up to 1913 K and then rapidly heated (20 K/s) to the desired temperature. A fast heating cycle was adopted between 1913 and 1963 K to minimize the time of reaction between the metal and rare earth oxide before melting. The temperature was held for 300 seconds before power was shut down. This procedure yields a cooling rate of ~1 K/s. The reacted titanium samples were then analyzed for oxygen and, in some cases, for the respective rare earth elements.

III. RESULTS AND DISCUSSION

A. *Effect of Rare Earth Oxide Face Coats on Metal-Mold Reaction*

1. *Microhardness profile and oxygen analysis*

The rare earth oxides studied were CeO_2, Sm_2O_3, Gd_2O_3, La_2O_3, Nd_2O_3, Y_2O_3, and didymium oxide ($Nd_2O_3 \cdot Pr_2O_3$). The selection was based on the free energy of formation of the oxides. Zirconia was also evaluated for comparison. The microhardness profiles of titanium rods cast in investment molds with different face coats are given in Figure 2. The microhardness profiles in the cast rods of all the studied oxides become invariant after a distance of about 550 μm.

It has been suggested earlier[19,20] that the relative difference in bulk hardness provides a good index of the relative stability of the molds. Higher bulk hardness indicates greater oxygen contamination. This is supported by the oxygen analysis obtained from the center of the rods (Table I). For comparison, the analysis of titanium buttons used as a charge for casting is also included in Table I. The hardness data estimated from the oxygen content using the correlation described earlier[19,20] are about 30 numbers lower than the measured value. The surface hardness also yields a similar sequence, except

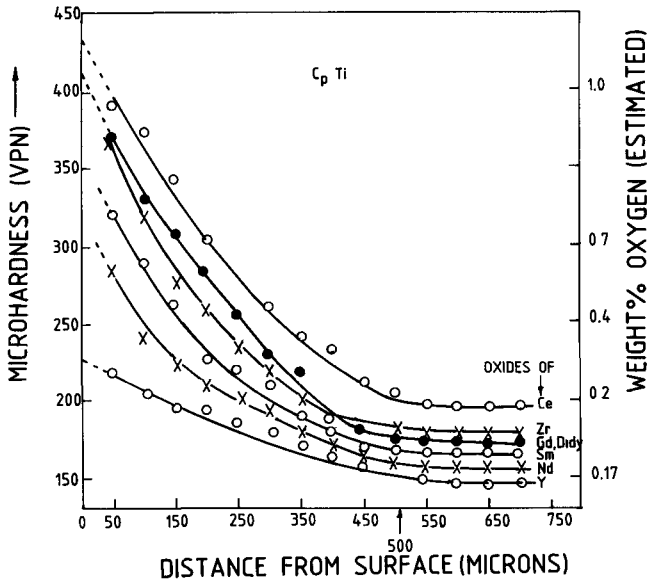

Fig. 2—Effect of rare earth oxide face coats on microhardness profile of investment cast titanium.

that ZrO_2 shows lower hardness than that of Gd_2O_3 and didymium oxide. Surface hardness, however, is also influenced to a high degree by the metallic constituents of the mold (*e.g.*, Zr, Nd, and Y). The increase of surface hardness is due to the continuation of diffusion of mold constituents even after the commencement of solidification. This is discussed in detail in Reference 19. Surface hardness cannot be considered as a very accurate measure of the extent of metal-mold reaction, because different metals have different hardening effects. Bulk hardness, which is more dependent on oxygen contamination, probably provides a better measure of the relative stability of oxides.

Metallic elements, in a few cases (ZrO_2, Nd_2O_3, and Y_2O_3 face coats), were also analyzed, and the metallic species were found to be present in quantities less than 0.1 pct. Thus, there should not be any significant hardening effect as a consequence of metallic contamination in the bulk. It may also be seen that mass balance between oxygen and the metallic constituent is not satisfied. The fact that increase in oxygen is much larger than corresponding values of metallic constituents suggests that metallic components are largely left behind in the mold as lower oxides or intermetallics of titanium. The mold oxides are not completely dissolved by liquid titanium.

Based on microhardness and oxygen analysis data, the oxides can be graded in the ascending order of their stability for titanium castings as follows:

$$CeO_2 \rightarrow ZrO_2 \rightarrow Gd_2O_3 \rightarrow \text{didymium oxide } (Nd_2O_3 \cdot Pr_2O_3) \rightarrow Sm_2O_3 \rightarrow Nd_2O_3 \rightarrow Y_2O_3$$

2. *Free energy and solid solubility*

The gradation of stability of rare earth oxides outlined above from experimental data cannot be fully explained by the standard free energy data for oxides. The level of contamination in liquid titanium from refractory oxides, however, may not only be related to thermodynamic stability of the oxide but may also be influenced by the solubility of the metallic species in titanium. The data on melting point, free energy of formation, and solubility for the various oxides studied are included in Table II.

It has been found empirically that Nd_2O_3 performs better than Gd_2O_3 and Sm_2O_3 (Table I) even though it has a slightly less negative energy of formation (~10 kJ/mol O_2) and lower melting point (80 K). The anomaly may be caused by solution effects. There are no data on Sm solubility in titanium. However, Gd exhibits a slightly higher solid solubility (7 wt pct at 1548 K) in titanium than Nd (6 wt pct at 1823 K). The higher solubility and lower activity of Gd may partly account for the observed superiority of Nd_2O_3 over Gd_2O_3. Didymium oxide performs better than Gd_2O_3 but inferior to Sm_2O_3. It is difficult to make any valid assumptions for didymium oxide in the absence of thermodynamic and solubility data. However, it is expected that its performance may be close to Nd_2O_3, which is the major constituent of this double oxide. It is observed that ZrO_2 performed better than CeO_2, and this is in accordance with the free energy of formation of oxides. Here, a higher solubility factor did

Table I. Bulk Oxygen Content and Hardness in Titanium Rods Cast in Investment Molds with Different Rare Earth Oxide Face Coats

Face Coat	Content of O and (Other Elements)* (ppm)	Equivalent Hardness[19] (VPN)	Measured Hardness (VPN)
CeO_2	2050	175	200
ZrO_2	1600 (Zr < 0.1 pct)*	150	180
Gd_2O_3	1510	145	175
Didymium oxide ($Nd_2O_3 \cdot Pr_2O_3$)	1460	140	175
Sm_2O_3	1250	130	165
Nd_2O_3	1140 (Nd < 0.1 pct)*	125	160
Y_2O_3	950 (Y < 0.1 pct)*	110	150
Ti buttons	800		100

not adversely influence the performance of ZrO_2, probably because of a larger difference in the free energy (40 kJ/mol O_2 at 2000 K) (Table II).

The above observations confirm the view that the level of contamination in titanium casting is not only related to thermodynamic stability of oxide (ΔG_f°) but it is also dependent on the solution effect. However, the solution effect is expected not to influence the thermodynamic stability of oxides if the difference in free energies of oxides is large. In the absence of sufficient thermodynamic data on solution of metal in titanium, it is difficult to predict accurately the behavior of oxides of stability.

3. *Diffusion profile for contaminants*

It has been demonstrated on earlier occasions that microhardness profiles are indicative of diffusion depth of oxygen. However, it is only an indirect evidence. Microprobe analysis is not very sensitive when the concentration of elements (particularly of lighter eleme is low. Therefore, attempts were made to evaluate depth profile for oxygen (Figure 3) and metallic spe (Figure 4) originating from the refractory oxide face c using SIMS. Three titanium samples cast in molds v face coats of either ZrO_2, Nd_2O_3, or Y_2O_3 were con ered for diffusion profile evaluation. In all of the ca signals for titanium were also recorded along with element of interest. The intensity counts for each ment were normalized with intensity counts of titani and the results are presented as $[I_i/I_{Ti}]$ *vs* depth in Figur The diffusion depth can be considered as the distanc which the profile for the element becomes invariant

The nature of the oxygen profiles (Figure 3) is sim to that of the microhardness profile (Figure 2). It is served that Y_2O_3 face coat causes less oxygen cont ination than observed in the cases of Nd_2O_3 and Zr The oxygen plots display a diffusion depth of ~550 μ which agrees well with the results of microhardness pl

Table II. Free Energy and Solubility Data of Various Rare Earth Oxides Used in This Study

Face Coat Oxide	Melting Point (K)	Standard Free Energy of Formation of Oxides, $-\Delta G^\circ$ (kJ/mol O_2)[9,21] 1000 K	2000 K	Maximum Solid Solubility (Wt Pct) of Rare Earth Element in β-Ti[21,24]
TiO	2003	994.2	705.8	—
TiO_2	2143	739.5	652.7	—
Y_2O_3	2683	1076.5	889.1	3.7 at 1628 K
ThO_2**	3573	1048.8	—	86.5 at 1463 K (eutectic composition)
Pr_2O_3†	2663	1023.2	834.6	*
Sm_2O_3	2593	1022.1	824.03	*
Gd_2O_3	2668	1021.95	835.74	7.0 at 1548 K
Nd_2O_3	2588	1013.0	823.05	6.0 at 1823 K
Didymium oxide	*	*	*	*
La_2O_3**	2573	1005.37	817.22	7.0 at 1823 K
ZrO_2	2963	899.56	716.6	complete solubility
CeO_2	2670	880.7	674.08	6.0 at 1723 K

*Data not available.
**Not studied for investment casting experiments.
†Data included since it is constituent of didymium oxide.

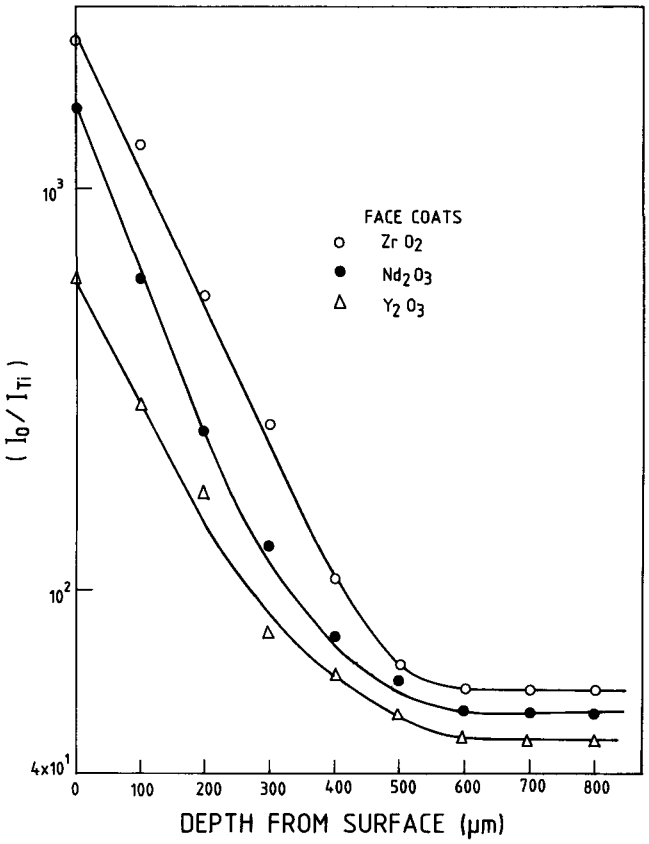

Fig. 3—Diffusion profile of oxygen as determined by SIMS.

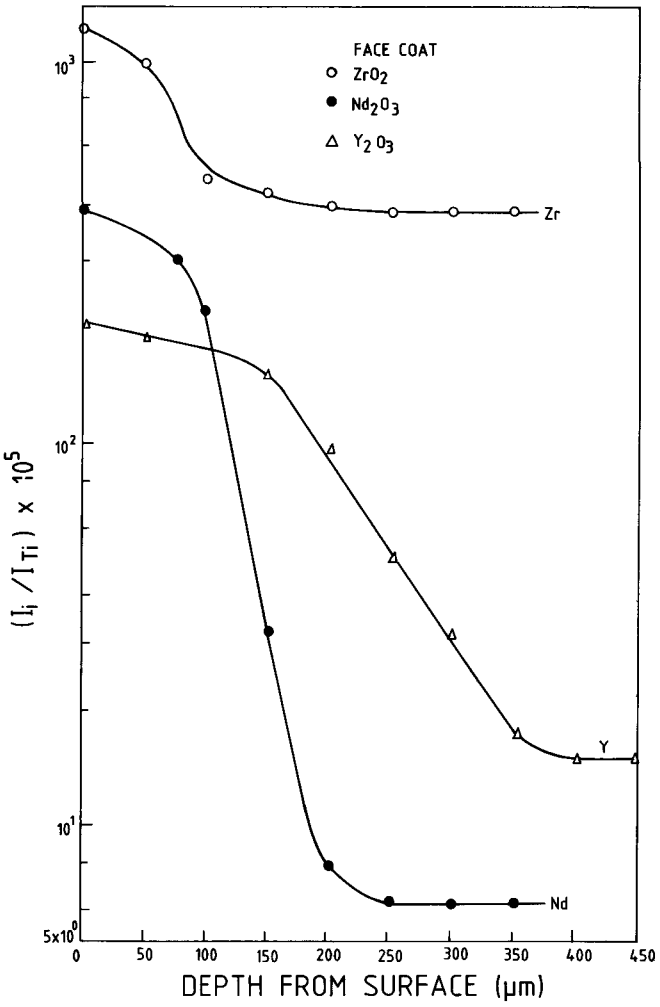

Fig. 4—Diffusion profile of metallic species of refractory oxides as determined by SIMS.

It is also observed that the diffusion depth for oxygen has remained constant irrespective of the type of face coat used; this again is in good accord with the microhardness results (Figure 2). The SIMS results on oxygen contamination confirm the earlier assumption that microhardness profile is representative of oxygen profile and the distance from the mold-metal interface at which the hardness attains a constant value corresponds to the diffusion depth for oxygen.[19,20]

The profile also shows that the oxygen diffusion is not dependent on the stability of the oxide. This again is in agreement with the results obtained with zircon sand molds which show that diffusion depth of solutes is not effected by the extent of metal-mold reaction. However, difference in depth of diffusion zone in investment cast rods (550 μm) and cast rods in zircon sand molds (700 μm)[20] has been noted. This is due to the faster cooling rate in investment cast rods. The wall thickness of the shell was 3 mm in investment molds, considerably smaller than 50 mm for sand molds.[20] These results indicate that the depth of the diffusion zone of oxygen is not dependent on the stability of mold oxides but influenced by the cooling rate of the casting.

The normalized line scans for Zr, Nd, and Y given in Figure 4 yield the diffusion depths of 200, 250, and 400 μm. The reasons for this variation are not clear at this time. Higher diffusion depth for Y as compared to Nd can be partly attributed to lower atomic radii of Y (17.9 nm)[21] as compared to that of Nd (18.2 nm).[21]

B. *Effect of Heating Titanium in Contact with Face Coat Oxides on Oxygen Contamination*

Another method for evaluating the relative stability of rare earth oxides in contact with liquid titanium is to heat these oxides along with titanium above its melting point (1941 K) and study the contamination levels. The experiments were carried out, as per Section II–D, at temperatures of 1943 (the melting point of titanium) and 1963 K. This test provided much more severe conditions for reaction than those occurring during casting experiments. This test, in fact, simulates more closely the conditions for crucible applications. After the experiment, the titanium rod was found to retain its original shape. In most of the cases, the surface appeared to have melted, and titanium samples displayed a shiny surface. The oxygen analysis of titanium was done in all of the cases. The results are given in Table III. The analytical results for metallic species in titanium from ZrO_2, Nd_2O_3, and Y_2O_3 are also included in Table III. It is seen that there is a positive increase in Zr in the titanium sample when heated in contact with ZrO_2, the values being 1.3 and 1.6 wt pct at 1943 and 1963 K, respectively. However, there was hardly any increase in the concentration of Nd

Table III. Analysis of Titanium Rods Heated along with Rare Earth Oxides above the Melting Point of Titanium

Oxides	Wt Pct Contamination of Titanium at 1943 K		1963 K	
	O	Other Elements	O	Other Elements
ZrO_2	6.0	Zr (1.3)	NA	Zr (1.6)
Sm_2O_3	3.23	NA	4.88	NA
Gd_2O_3	2.30	NA	2.96	NA
La_2O_3	1.76	NA	2.1	NA
Didymium oxide	1.5	NA	1.88	NA
Nd_2O_3	1.3	Nd (ND)	1.5	Nd (<0.1)
ThO_2	1.20	NA	1.4	NA
Y_2O_3	0.85	Y (ND)	1.10	Y (0.05)

ND = not detected.
NA = not analyzed.

or Y in the titanium sample when heated in contact with Nd_2O_3 and Y_2O_3 oxides. The above observations support the earlier findings[19,20] that the mold oxides do not completely dissolve in the liquid titanium and the metallic components are left behind in the molds, probably as lower oxides. From the oxygen analysis, the stability of oxides can be graded in increasing order as follows:

$$ZrO_2 \rightarrow Sm_2O_3 \rightarrow Gd_2O_3 \rightarrow La_2O_3$$

$$\rightarrow \text{didymium oxide} \rightarrow Nd_2O_3 \rightarrow Y_2O_3$$

The order of stability of rare earth oxides evaluated by this approach is similar to that found from experiments with investment molds (Section III–A) with rare earth oxide face coats. The positions of Y_2O_3 and Nd_2O_3 remain the same as in the previous experiment. However, the performance of Sm_2O_3 appears to have deteriorated below those of didymium oxide and Gd_2O_3. Since the increase in the standard Gibbs energy of formation of Sm_2O_3 with temperature is steeper than for Gd_2O_3, it is expected that the performance of Gd_2O_3 at higher temperatures will be inferior. However, the performances of both of these oxides have been found to be inferior to that of La_2O_3 in this experiment, where oxide and metal were heated above the melting point of titanium. This is not expected purely from a thermodynamic point of view. The experimental results suggest that kinetic factors are also important in determining the extent of contamination, when thermodynamic stability is comparable.

Among the oxides tested, Y_2O_3 and Nd_2O_3 are found to be least reactive. However, because of its low cost, didymium oxide ($Nd_2O_3 \cdot Pr_2O_3$) can be considered as an economical face coat for investment casting of titanium.

C. *Thermodynamics of Metal-Mold Reactions*

Thermodynamic calculations have been carried out in order to determine solubility of Y_2O_3 and ZrO_2 in molten titanium and correlated with experimental results.

1. *Solubility of Y_2O_3*

Based on the standard Gibbs energy of formation of Y_2O_3 and Gibbs energy of solution of oxygen and yttrium in liquid titanium, the solubility product of mol titanium has been evaluated by Hoch[22] as

$$T \ln \text{wt pct Y} + 1.5T \ln \text{wt pct O} = -19.9 + 8.325$$

where T is temperature in kilo Kelvin (kK). The sc bility product can be calculated thermodynamically desired temperatures by rearranging the above equati

$$[\text{wt pct Y}]\,[\text{wt pct O}]^{1.5} = \exp\,[-(19.9/T) + 8.32$$

At the experimental temperature of 1.963 kK, the ubility product is

$$[\text{wt pct Y}]\,[\text{wt pct O}]^{1.5} = 0.163$$

From Table III, at 1963 K, the experimental solubilities

$$\text{wt pct Y} = 0.05 \quad \text{and wt pct O} = 1.1$$

$$(\text{solubility product})_{exp} = [0.05]\,[1.1]^{1.5} = 0.0577$$

The experimental value (0.0577) is lower than computed value (0.163). This is expected since equi rium is probably not reached in the short time 300 seconds at 1963 K. However, an order of ma tude agreement is achieved.

2. *Solubility of ZrO_2*

Solubility of ZrO_2 has been calculated assuming ic mixing of Zr in Ti in the liquid state.

$$Zr\,(s) + O_2\,(g) \rightarrow ZrO_2\,(s)$$

The standard free energy for this reaction is given JANAF:[23]

$$\Delta G^\circ = -259 + 42.9T \quad \text{kcal/mol}$$

$$\text{or} = -1084 + 179.5T \quad \text{kJ/mol}$$

$$\text{or} = -RT \ln K$$

where T is temperature in kilo Kelvin. Rearran Eq. [7],

$$\ln K = -\Delta G^\circ/RT = (1084/RT) - (179.5/R)$$

where K is the equilibrium constant for Reaction [6

The dissolution of ZrO_2 in liquid titanium is given

$$\underline{Zr} + 2\underline{O} \rightleftharpoons ZrO_2\,(s)$$

where $\underline{Zr}$ and $\underline{O}$ denote Zr and O in liquid titanium. F the equilibrium constant,

$$K = (a_{ZrO_2}/a_{\underline{Zr}} \cdot (a_{\underline{O}})^2)$$

where $a_{ZrO} = 1$, Eq. [10] can be rewritten as

$$\ln K = -\ln a_{\underline{Zr}} - 2 \ln a_{\underline{O}}$$

From the literature, we have[22]

$$\ln a_{\underline{O}} = \ln (\text{wt pct O}) - (65.27/T) + 9.528$$

where the activity of dissolved oxygen is expressed reference to the diatomic gas as the standard state.

For

$$Zr\,(s) \rightarrow Zr\,(l)$$

$$\Delta G^\circ\,[13] = \Delta H_f\,(1 - T/T_m)$$

where ΔH_f is the heat of fusion of Zr (19.3 kJ/mol) and T_m is the melting point of Zr (2.12 kK). Substituting these values in Eq. [14], we get

$$\Delta G^\circ\,[13] = 19.3 - 9.08T \qquad [15]$$

Assuming ideal mixing of Zr in liquid state,

$$\text{Zr (l)} \rightarrow \text{Zr (alloy)} \qquad [16]$$

$$\Delta \bar{G}_{Zr} = RT \ln X_{Zr} \qquad [17]$$

Therefore, for the reaction

$$\text{Zr (s)} \rightarrow \text{Zr (alloy)} \qquad [18]$$

$$\Delta G^\circ\,[18] = RT \ln a_{Zr} = \Delta G^\circ\,[13] + \Delta \bar{G}_{Zr}\,[17]$$

$$= (19.3 - 9.08T) + RT \ln X_{Zr} \qquad [19]$$

where X_{Zr} = [wt pct Zr/(100 at. wt Zr)] × at. wt Ti = wt pct Zr · (47.90/9122) for dilute solution of Zr in Ti. Therefore,

$$\ln X_{Zr} = \ln (\text{wt pct Zr}) - 5.2493 \qquad [20]$$

Substituting for $\ln X_{Zr}$ in Eq. [19] and dividing the whole expression by RT,

$$\ln a_{Zr} = \ln (\text{wt pct Zr}) - 5.2493 + (19.3/RT) - (9.08/R) \qquad [21]$$

Substituting values of $\ln a_O$ [12] and $\ln a_{Zr}$ [21] in Eq. [11] and combining it with Eq. [8], we get

$$\ln K = -\ln (\text{wt pct Zr}) + 5.2493 - (19.3/RT) + (9.08/R) - 2 \ln [\text{wt pct O}] + (130.54/T) - 19.056 = (1084/RT) - (179.5/R) \qquad [22]$$

Rearranging Eq. [22], one gets

$$\ln (\text{wt pct Zn}) + 2 \ln (\text{wt pct O}) = 5.2493 - (19.3/RT) + (9.08/R) + (13.054/T) - 19.056 - (1084/RT) + (179.5/R) \qquad [23]$$

where R is the gas constant (8.314 kJ/mol kK).

$$\ln (\text{wt pct Zr}) + 2 \ln (\text{wt pct O}) = -(2.1639/T) + 8.8755 \qquad [24]$$

$$(\text{wt pct Zr}) \cdot (\text{wt pct O})^2 = \exp [-(2.1639/T) + 8.8755] \qquad [25]$$

The computed solubility product at a temperature of 1.963 kK is

$$[(\text{wt pct Zr}) (\text{wt pct O})^2] = 2376 \qquad [26]$$

Knowing the measured concentrations of oxygen (7.3 wt pct) and zirconium (1.6 wt pct) in titanium in contact with ZrO_2 at 1963 K, the solubility product is

$$(\text{solubility product})_{exp} = [(1.6)\,(7.3)^2] = 85.26 \qquad [27]$$

The value of the experimental solubility product for ZrO_2 is much lower than the thermodynamically computed value of 2376. There are two possible reasons for this discrepancy:

(1) As oxygen dissolves in titanium from ZrO_2, the melting point of Ti increases. At a composition corresponding to 73 wt pct dissolved oxygen in titanium, the liquidus and solidus temperatures are 2153 and 2113 K, respectively.[24] Dissolution of oxygen therefore moves the alloy from a liquid to solid state. Once the solid is formed, diffusion rates are slow, and the rate of dissolution is significantly retarded. Therefore, the measured solubility product is significantly below the value computed thermodynamically.

(2) Since the computed solubility product of ZrO_2 is very large, a significant amount of oxide has to dissolve at equilibrium. Obviously, 300 seconds is not sufficient for dissolving the equilibrium concentration of the oxide.

IV. CONCLUSIONS

1. The relative stability of rare earth oxides can be obtained by determination of microhardness profile and bulk oxygen in cast titanium rods under standardized conditions. These experiments provide semiquantitative evaluation on the relative stability of oxides.
2. The microhardness profile provides an index for the evaluation of the relative stability of the oxide. Lower bulk hardness or oxygen content is indicative of higher stability of the face coat oxide.
3. The distance from the surface at which the invariant portion of the microhardness profile begins was found to be a constant (550 μm), irrespective of the face coat oxide used, under similar casting conditions.
4. The intensity profiles of oxygen, normalized with respect to titanium, are similar to microhardness profiles. The gradation of oxides, based on the oxygen profile, in increasing order of their stability is $ZrO_2 \rightarrow Nd_2O_3 \rightarrow Y_2O_3$.
5. Based on the bulk hardness and oxygen analysis of 20-mm cast rods in investment molds (Figure 2 and Table I), the oxides can be graded in order of increasing stability as

$$CeO_2 \rightarrow ZrO_2 \rightarrow Gd_2O_3 \rightarrow \text{didymium oxide} \rightarrow Sm_2O_3 \rightarrow Nd_2O_3 \rightarrow Y_2O_3$$

6. The grading does not fully follow the free energy data on the formation of these oxides. A better correlation with experimental finding is obtained when the solubility of the metallic species in titanium is also taken into consideration.
7. In more severe conditions, where titanium was heated above its melting point in contact with face coat oxides, the observed contamination levels suggest a slightly different sequence of stability for the oxides:

$$ZrO_2 \rightarrow Sm_2O_3 \rightarrow Gd_2O_3 \rightarrow La_2O_3 \rightarrow \text{didymium oxide} \rightarrow Nd_2O_3 \rightarrow Y_2O_3$$

8. The fact that the oxygen contamination is much higher than that of the metallic constituent of the oxide confirms that refractory oxides are not completely leached by liquid titanium. Oxygen is preferably transferred

to the liquid titanium, leaving behind the metallic components as lower oxides in the mold.

9. The observed solubility of Y_2O_3 correlates with thermodynamic data for the oxide and free energy of solution of oxygen and yttrium in titanium. Similar calculation for ZrO_2 is less satisfactory. Liquid titanium solidifies as a significant amount of oxygen is picked up isothermally from the oxides.

REFERENCES

1. J.C. Baily: *Br. Foundryman*, 1960, vol. 53, pp. 187-96.
2. A. Short: *Br. Foundryman*, 1961, vol. 54, pp. 400-09.
3. J.B. Cains: *Trans. Am. Foundrymen's Soc.*, 1963, vol. 77, p. 111.
4. L.W. Eastwood and C.M. Craighead: Air Force Materials Laboratory, OH, AFML-TR-6218, Part I, 1950.
5. M. Grafinkle and H.M. David: *ASM Trans.*, 1965, vol. 58, pp. 520-30.
6. S.A. Klevtsur and V.V. Sagalovick: *Zashch. Pokrytiya Met.*, 1972, no. 6, p. 165.
7. R.A. Brown: U.S. Patent No. 3,743,003 (CI.164/16 B22C), Rem Metals Corporation, Albany, OR, 1973.
8. R.D. Waldron: U.S. Patent No. 4,104,706 (CI.106-55, CO 4B 35/00), Research Enterprises Corporation, Phoenix, AZ, 1977.
9. K.A. Gschneidner, Jr., N. Kippenhan, and O.D. McMasters: *Thermochemistry of the Rare Earths*, Rare Earth Information Center, Ames, IA, 1973.
10. L.G. McCoy: Air Force Materials Laboratory, OH, AFML-TR-72-238, Part II, 1974.
11. D.R. Schuyler, J.A. Petrusha, G.S. Hall, and S.R. Seagle: Air Force Materials Laboratory, OH, AFML-TR-76-80, 1976.
12. B.C. Weber, W.M. Thompson, H.O. Bielstein, and M. Schwartz: *J. Am. Ceram. Soc.*, 1957, vol. 40, pp. 363-73.
13. E.J. Chapin and W.H. Friske: Naval Research Laboratory, W NRL Report 4467, Part I, 1954; NRL Report 4478, Part II, 19.
14. C.A. Alexander: Air Force Materials Laboratory, OH, AFM TR-72-238, 1972.
15. S.R. Lyon and S. Inouye: in *The Interaction of Ti With Refr tory Oxides, Titanium Science and Technology*, R.I. Jaffee : H.M. Burte, eds., Plenum Press, New York, NY, 19 pp. 271-84.
16. R.L. Helferich and R.L. Zanis: Naval Ship Research and I velopment Center, MD, NSRDC Report No. 3911, 19 3.
17. S.J. Hayden and M.J. Blackburn: 2nd Annual Report, Aerosp Research Laboratories, Wright-Patterson Air Force Base, Dayt OH, 1975, Contract No. AF-32615-74-C-1140.
18. D. Mukherji, R.L. Saha, and C.R. Chakravorty: *Trans. Ina Inst. Met.*, 1985, vol. 38, pp. 465-71.
19. R.L. Saha, T.K. Nandy, R.D.K. Misra, and K.T. Jacob: *B Mater. Sci.*, 1989, vol. 12, p. 481.
20. R.L. Saha, T.K. Nandy, R.D.K. Misra, and K.T. Jacob: *Tra Am. Foundrymen's Soc.*, 1990, in press.
21. E.A. Brandes: *Smithells Metals Handbook*, Butterworth's, Lond 1983.
22. M. Hoch: in *Solubility of Y_2O_3 in Liquid and Solid Ti ana Alloys, Titanium Science and Technology*, G. Lutjeri V. Zwicker, and W. Bunk, eds., Deutsche Gesellschaft f Metallkunde, Oberursel, Federal Republic of Germany, 19 pp. 1431-38.
23. *JANAF Thermochemical Tables*, National Bureau of Standar U.S. Dept. of Commerce, Michigan, 1971.
24. *Binary Alloy Phase Diagrams*, T.B. Massalski, ed., ASM, Me Park, OH, 1986.